UNIVERSITY OF
BATH

University of Bath

Variable stroke timing of rubber fins' duty cycle improves force

Keri M. Collins, Jennifer C. Brown, Ryan R. Ladd, Lily D. Chambers, Adrian Bowyer and William M. Megill[1]

Abstract - **Swimming animals can tune their kinematics to achieve increased propulsive performance. To engineer effective propulsive mechanisms, a better correlation between kinematics and dynamics is required in artificial designs. Two rubber fins: one with a NACA aerofoil shape, the other with a biomimetic shape, were used in two asymmetric oscillations in a static water tank. The force generation patterns within the parameter space and the response to the change in stroke timing, were dependant on the fin. The biomimetic fin produced peak force at a similar frequency and amplitude regardless of its kinematics and duty cycle. The response of the NACA fin, however, was dependent on the duty cycle. For the NACA fin, the fast-to-centreline kinematics caused larger resultant force over a narrow range of frequencies. For the fast-to-maximum-amplitude stroke, a lower resultant force was achieved, but over a larger range of frequencies. Digital Particle Image Velocimetry (DPIV) analysis showed the wake pattern of shed vortices. We present experiments and qualitative flow analysis that relate kinematic parameters, particularly the trailing-edge angle to resultant forces.**

I. INTRODUCTION

Swimming fishes with paired fins such as rays and skates often use asymmetric strokes of their appendages, with one half of the stroke faster than the other. Some ray species have a preferred frequency of oscillation of their large pectoral fins and elect to increase the speed of the upstroke in order to increase forward speed [1,2]. Unlike birds, fishes do not generally need to create lift so the reason for variable stroke timing is unclear. Investigations into tail-vortex interactions for carangiform swimming fish such as trout [3] suggest that a fish may destroy a shed vortex on the return stroke of the tail, thus extracting energy from its wake and increasing thrust. The vortices that are shed into the wake are formed by the movement of the fish tail from the midline towards the maximum amplitude. The movement from the maximum amplitude to the midline of the fish, which may destroy these vortices, is then the power stroke. With increased trailing edge velocity linked to increased vortex strength [4], it is our hypothesis that by changing the speed of oscillation through the quarter periods, force production of two different rubber fins will be modified.

II. METHODS

High-speed-camera and force-plate measurements of these two 120 mm fin forms were made. The speed of each quarter stroke was varied to create a fast-to-centreline and a fast-to-maximum-amplitude kinematic profile based on sinusoidal motion. Each oscillation set consisted of eight frequencies (0.5 Hz – 4.0 Hz) and four demand amplitudes (4° to 16°, in steps of 4°). The asymmetric oscillations altered the trailing edge angle and velocity in each quarter period.

A. Fins used

Following from the work of Riggs [5], a NACA0012 profile and a biomimetic (BIO) fin were cast in silicone rubber (Silastic 3483, tensile strength 3.5 MPa, 600% elongation at failure, Nottcutt, UK). Both fins were cast to have the same planform dimensions (0.012 m square) and an aspect ratio of one. The fins were cast directly onto their driving shafts. Thread woven around the shaft and glued in place allowed a good bond between the fin and the shaft.
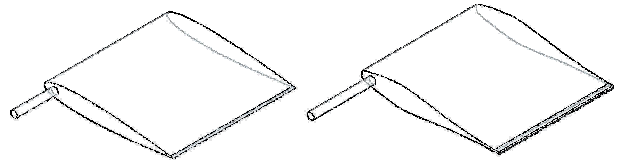
Fig. 1 Fin shapes used in the experiments *left:* the NACA0012 profile, *right*: the biomimetic profile, shown as cast onto the drive shafts.

The biomimetic fin was a modification of the standard NACA profile for which the section has been changed to represent the gross stiffness profile of a Pumpkinseed Sunfish (*Lepomis gibbosus*) [6]. The data for this stiffness, taken from [7], were used to change the profile based on the equation of the second moment of area, I:

$$I = bd^3/12 \qquad [m^4]$$

where b and d are the local section breadth (0.012 m) and depth respectively (various). The actual value of stiffness of the fish was scaled to create a fin of a similar width to the NACA fin. This produced a profile that was thicker just after the leading edge than the NACA0012 but thinner towards the trailing edge, as shown in Fig. 1.

B. Parameter space & waveforms

The generic oscillation of the fins was that of a sine wave. To introduce the quarter-period asymmetry, the time taken to the outside profile (FTO) and to 42.5% of T for the fast to the middle (FTM) profile. The shape of each quarter-period input waveform is still described by a sinusoid, Fig. 3. The time taken to complete one full oscillation at a given frequency setting remained the same for all the profiles. All references to frequency, f, in this paper describe the reciprocal of the time taken to complete one full oscillation.

The fins were oscillated in pure pitch at 4°, 8°, 12° and 16°, at frequencies ranging from 0.5 Hz to 4.0 Hz (in increments of 0.5 Hz) in the three kinematic modes: symmetric, FTO and FTM.
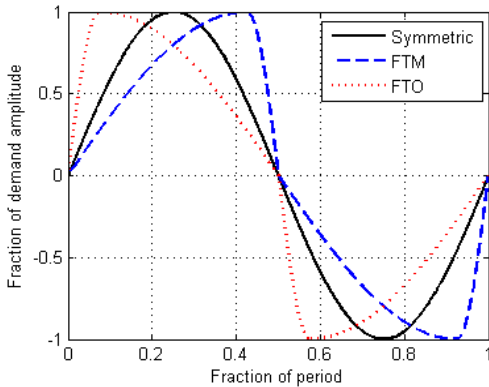

Fig. 3 Kinematics investigated are variations of a sine wave with the speed of the quarter period modified to be fast to the middle (FTM) or fast to the outside (FTO).

C. Kinematics set-up

The oscillating mechanism was a servo motor (Hitec HS-6965HB Hi-Speed Coreless), controlled through a micro-serial servo controller (Pololu, SSC03A). The apparatus was mounted on a rigid aluminium frame. The servo motor output arm was mechanically connected to a potentiometer (Spectrol, 357-0-0-103), which measured the real angle of the fin shaft. The smallest angle resolvable by the potentiometer was 0.7°. This removed measurement errors due to any inadequacies in the response of the servo to demand. The water moved by the fin increased the loading on the motor, and the higher frequency and amplitude combinations were out of the range of the servo. In these cases, the servo kept the frequency the same but restricted the amplitude. References to amplitude here specify if it is the real value or the input value.

The oscillator frame was mounted on a clear-walled static water tank with a working section of 0.3 m x 0.3 m x 1.3 m. Images of the fin were taken at 100 fps by a PCO camera that imaged the fin from underneath via a mirror set at 45° to both the underside of the tank and the camera.

The videos were analysed using LabVIEW and comprised two stages: first the outline of the fin in each frame was found and the midline was extracted as the point-by-point average of the two sides. Next the kinematic parameters

complete the portion of the stroke from the centre of oscillation to the maximum amplitude was changed from 25% of the total stroke time, T, to 7.5% of T for the fast to

were found based on the midlines. Parameters tested for correlation with produced force were trailing edge excursion, trailing edge angle and trailing edge velocity, where the trailing edge was defined as the final 6% of the fin.

D. Force rig design

To measure the forces produced in the x-y plane, experiments were conducted in a static water tank (1.60 m x 0.92 m x 0.70 m), which was found to have no effect on the force readings of the experiments. The oscillating mechanism rested on a pin at the rear and on three force sensors (Sensortechnics FSS1500NSB) at the forward end of the force bed, which was suspended over the tank via a rigid metal frame. One sensor was orientated in the z-direction (on the negative x side of the rig) and two sensors at ±45° to the z-axis (on the positive x side of the rig), as shown in Fig. 2. The sign convention is shown by the axes in the figure and the origin of these axes was coincident with the rear contact point.
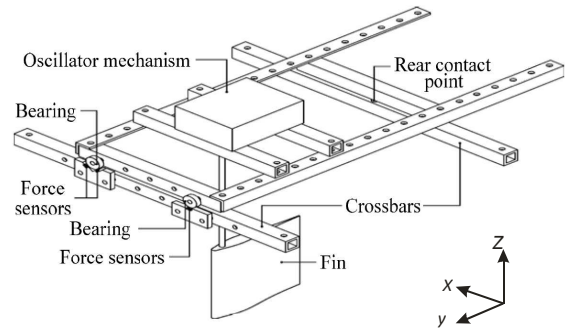

Fig. 2 The crossbars of the rig as suspended over the tank and the oscillating mechanism is rested on top; at the rear on a spike and at the forward end on three force sensors. Axes show the sign convention used with the origin coincident with the rear contact point. Taken and adapted from [5].

In its static state, the rig was loaded so that the sensors recorded a value in the middle of their range (~7.5 N). A PureBASIC program controlled the servo motor and the communications with the data acquisition box (PMD 1208FS, Measurement Computing). Force data analysis was conducted using MATLAB.

E. Digital particle image velocimetry (DPIV)

Flow visualisation was achieved by using DPIV. A (532 nm) laser light sheet of 1 mm thickness was used to illuminate neutrally buoyant seeded particles (Vestosint 1301, mean diameter 100 µm) in the water column. A high speed PCO camera was used to capture double images (1700 µs time delay) at 200 Hz through a 45° mirror. The particles were tracked between the double images to produce velocity vectors using Insight 3G (TSI Instruments).

2

III. Results

There are three elements to the experiments presented here. First, the force produced by the new kinematics is presented for each fin. Next, the kinematics are examined in more detail and related to the force to look for correlation. Finally, DPIV images accompany the kinematics to explain the force experiment results using wake analysis.

A. Force experiments

Modifications to the kinematics can be seen to alter the response of the fins in the parameter space in different ways. Fig. 4 shows the data for each fin in each kinematic configuration, with a symmetric response shown for comparison. The difference between the fins' response using the symmetric kinematic profile was demonstrated by Riggs [5]. Fig. 4 shows that the BIO fin appears less affected by the change in kinematics than the NACA fin. When using the FTO kinematics at a given demand amplitude, the force produced remains similar for increasing frequency – there is not the peak and trough that appears
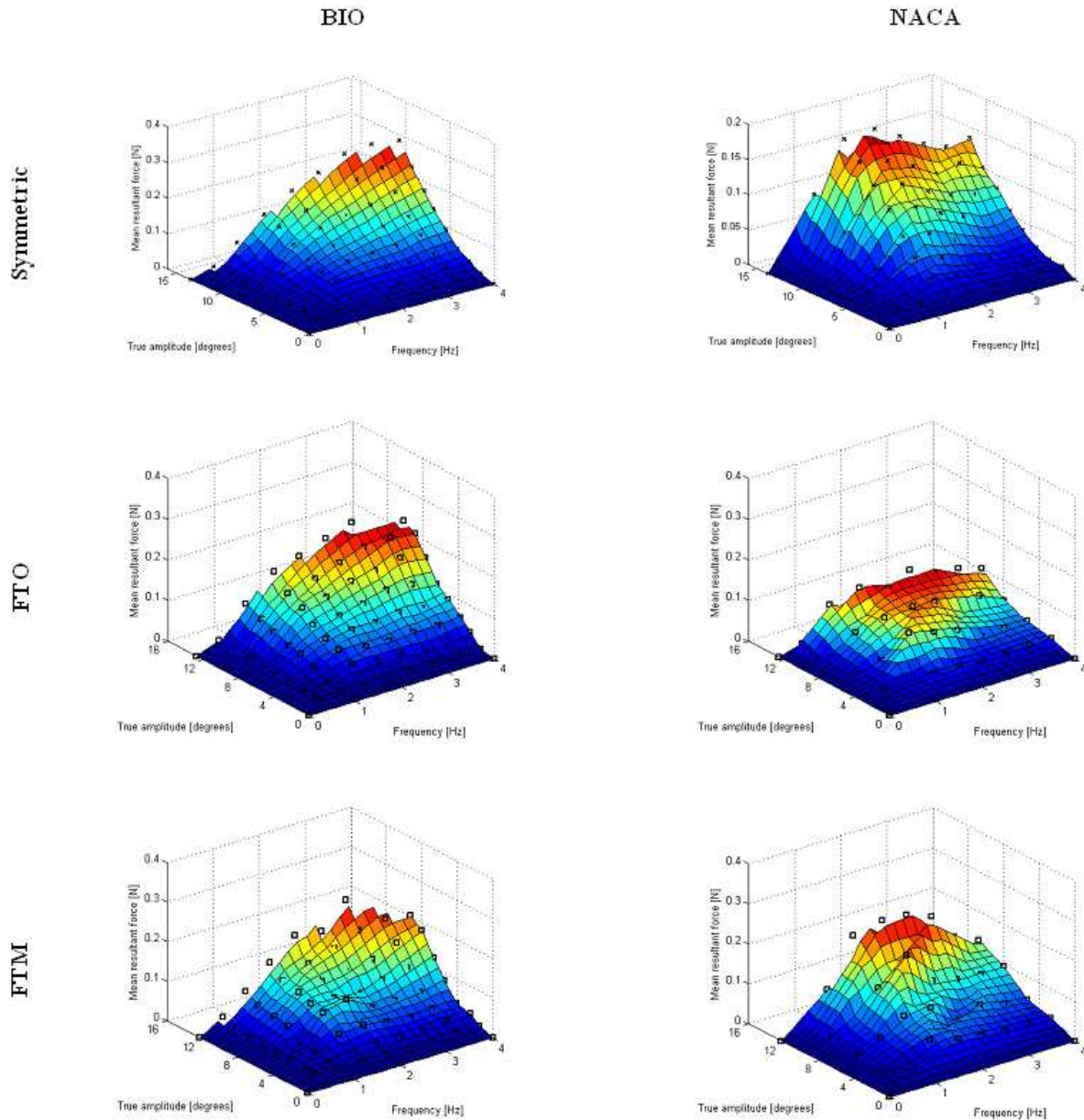
Fig. 4 Resultant force as imaged in the parameter space. These surfaces are the linearly interpolated surfaces through 32 unique combinations of frequency and demand amplitude (64 for the BIO fin and the two symmetric graphs). The overall response to the change in kinematics of each fin is different: the BIO fin's response is little affected, whereas the NACA fin's behaviour in the parameter space is seen to vary. The symmetric data are the mean of at least four experiments comprising 12 cycles each, however, the FTO and FTM represent only one experiment (12 cycles).

3

when using the symmetric kinematics. The FTM kinematics change the response of the NACA fin, making it more specialised. In this case, the frequency dependent peak is shifted to a higher frequency and the force value at this peak may be larger than in the symmetric case (symmetric force values are the mean of five experiments, FTO and FTM represent just one experiment). The FTM force is certainly higher than the force at the same frequency and demand amplitude for the FTO kinematics. After this peak, force production declines quickly as frequency increases past this point.

B. Kinematics and force

The second stage of experimentation was to link the dynamic geometry of the fin throughout the stroke with the force produced. The swimming speed of an oscillating rubber fish has been positively correlated with wave speed and tailbeat amplitude, which in turn are related to the control variables of body stiffness, driving frequency and driving amplitude [7]. Using a tethered fin, we can only relate the kinematics to bollard force rather than swimming

speed, but we find that across the same experimental range as [7] we get similar results.

The performance of the two fins using the symmetric kinematics across the parameter space has already been discussed [5] and the link to their kinematics is explored further [8].

Trailing edge excursion, shown to positively affect swimming speed of oscillating rubber fins [7], was found to correlate positively with force produced only if the driving frequency was constant. In this case, the trailing edge excursion was increased by increasing the input amplitude. This was true for both fins in each of the three kinematic patterns - symmetric, FTO and FTM.

Following the hypothesis of vortex destruction by the return stroke of a fish tail [3], Fig. 5 shows the force produced as a function of average maximum trailing edge angle for both fins in the three kinematic profiles. The average maximum trailing edge angle is the mean value of the maximum positive and the maximum negative angle and so considers both halves of the stroke. In the symmetric
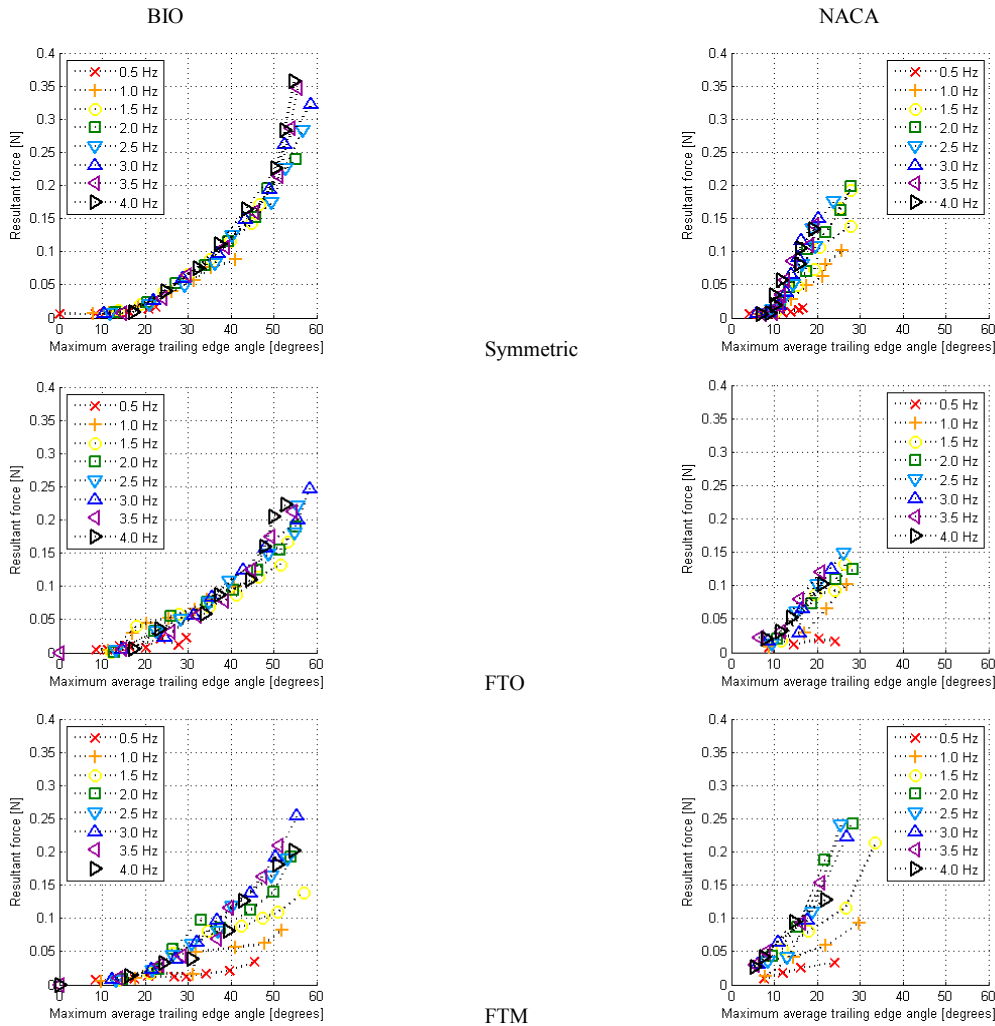

Fig. 5 Average maximum trailing edge angle relative to the horizontal axis of the flow channel is a good predictor of average resultant force produced by both fins using all three types of input kinematics (symmetric, FTM and FTO) across the range of experimental frequencies. Average maximum trailing edge angle is based on the final 6% of the fin during one oscillation.

case, for both fins, the trailing edge angle shows little dependence on the frequency of oscillation with all points falling onto the same approximate curve, dependent on the fin used. The FTM stroke obeys this trend at frequencies of 2.0 Hz and above. Below this, the frequency is shown to have an effect on the force produced on both the BIO and the NACA fin, and this is shown as the separation of data at these frequencies in Fig. 5. The lower frequencies produce trailing edge angles consistent with the rest of the data, but force production is lower. The FTO kinematics provokes a force response that is similar to that of the FTM, though only the lowest frequency deviates from the main curve.

Trailing edge velocity was found to be weakly correlated with force in every case, but values within frequency groups were subject to large fluctuations. Further repetitions of the experiments may be necessary to uncover the relationship between trailing edge velocity and force production.

C. DPIV and kinematics

It is evident in the velocity magnitude plots that for both fins, regardless of the stroke timing, higher frequencies caused larger wake velocity, a result that corroborates the resultant force calculations.

For the BIO fin, the paired vortices indicative of a reverse Kármán vortex street was obvious in the FTO wake pattern but are not in the FTM data. The velocity profile illustrated that the wake of the FTM fin was low and in the same axis as the fin. Conversely, the FTO fin wake was laterally displaced as discrete domains of accelerated fluid. The magnitude of the wake velocity describes the flow in the negative y direction, as defined in Fig. 2, as averaged over one cycle. For the BIO fin, this was similar for the three kinematic profiles at a given frequency.

Using the NACA fin at a frequency of 1.5 Hz, the average wake velocity magnitude was highest behind the symmetrically flapping fin. There was evidence that the wake velocity magnitude was higher resulting from the FTM

Fig. 6 Vorticity plot of NACA fin at 1.5 Hz, clockwise rotation (blue) and anticlockwise (red) rotation of the fluid. The overlaid arrow shows the direction of movement of the vortex pair.

kinematics than the FTO kinematics, but more experiments are needed to confirm this. The wake patterns, Fig. 6, show that for the FTO kinematics, a pair of vortices was shed at an angle to the fin, as indicated by the large arrow in the figure. The wake patterns behind the fin using the FTM kinematics showed a single vortex per half cycle being shed, that moved downstream at no discernible angle.

IV. DISCUSSION

Oscillating symmetrically, the BIO fin produced more force as the frequency increased, whereas the NACA fin exhibited a peak in force production at lower frequency. Variable stroke timing did not alter these trends but did change the magnitude of the force response for the NACA fin.

The NACA fin produced a greater resultant force at $f = 1.5$ Hz than at $f = 4.0$ Hz for the new duty cycles investigated. This decrease in force corresponds with results for the NACA fin oscillating symmetrically [6]. At $f = 1.5$ Hz and using the FTM kinematics, the NACA fin produced a greater resultant force than the NACA fin with symmetric or FTO kinematics.

The BIO fin produced more force at high frequency than at low frequency. Adjusting the stroke timing did not affect the force in a statistically significant manner, based on the maximum standard deviation of the resultant force produced by the BIO fin oscillating symmetrically ($n = 4$ experiments).

The local stiffness of the fins is directly proportional to the sectional depth. The results of varying stiffness profile indicate that trailing edge angle is an important parameter to relate the fin kinematics to the force produced. Since the BIO fin had a lower stiffness towards its trailing edge than the NACA fin, it deflected more in response to the input kinematics, shown by the larger trailing edge angles achieved (Fig. 5).

The wakes behind the FTM profiles for both fins were estimated to be narrower than those resulting from the FTO kinematics. DPIV analysis showed the oblique movement of the vortices. Taking the ratio of maximum average thrust to maximum average lateral force as a measure of the usefulness of the forces produced, the NACA FTM kinematics produced larger values than FTO (FTM: 0.49, FTO: 0.30). From this we infer the ratio of downstream to cross-stream flow in the wake, which suggests the proportion of the hydrodynamic force available for forward propulsion.

A limitation of our approach is that the various stages of the experiment were not conducted concurrently. One way to better link the kinematics with the dynamics would be to conduct the experiments concurrently and to increase their number. Further consideration of the development of the wake patterns and the vortex structures would better describe the fluid-structure interaction of the two fins.

Introducing flexibility to oscillating fins creates a delay of the input kinematics from the leading edge to the trailing
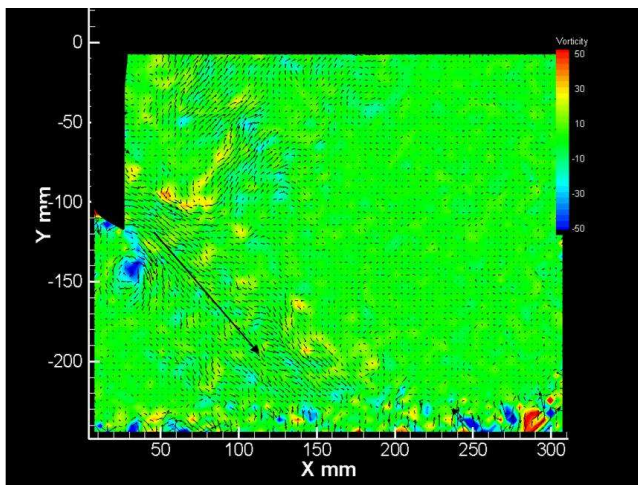
edge, modifying the trailing edge amplitude. As trailing edge excursion increases at a given frequency, vortex strength and hence thrust, is increased [4]. The NACA fin conforms to this; the trailing edge excursion and the resultant force were higher (for all kinematics) at $f = 1.5$ Hz than at $f = 4.0$ Hz. The BIO fin did not behave in the same way. As the frequency was increased, the trailing edge excursion decreased but the resultant force was higher. Our results suggest that this design is able to withstand perturbations to the input kinematics. Further study is underway to ascertain how the dynamic geometry of the BIO fin relates to its force production.

Trailing edge excursion has been used in the literature [7] to relate kinematics to force produced, but it did not adequately describe the force over the parameter space used in these experiments. Trailing edge angle was found to correlate with resultant force across all fins and kinematics throughout the parameter space.

In swimming fish, the movement of the tail from its maximum amplitude towards the body midline has been described as the power stroke [3]. In this study, the location of the maximum trailing edge angle occured at a different point of the power stroke of the FTM and of the FTO kinematics at $f = 1.5$ Hz (Fig. 7). For the NACA and the BIO fins using the FTO kinematics, the maximum trailing edge angle was found at the end of the power stroke, i.e. when the trailing edge returns to the midline. For the FTM kinematics, the maximum trailing edge angle occurred at the beginning of the power stroke, i.e. just after the maximum trailing edge excursion. This means that the time between the maximum angle and the trailing edge being parallel to the longitudinal axis is longer during the FTM stroke. This further implies that during the power stroke a larger downstream force could be generated, as supported by the increased velocity magnitude in the wake.

V. Conclusions

The BIO fin did not alter its force production with a change in duty cycle, suggesting it behaved as a generalist in response to varying stroke timing. This could have applications for its use in unsteady hydrodynamic environments in which demand kinematics may be subject to perturbations. Altering the stroke timing of two flexible fins' duty cycles was found to modify the resultant force magnitude produced in the NACA fin.

Trailing edge angle was found to be a good predictor of force produced. From here a simple mass-spring-damper model can be made to recreate the kinematics of the fins under the same input conditions. The prediction of parameters that would create large propulsive forces would require searching for input kinematics that maximised trailing edge angle during the power stroke.

Furthermore, with a more comprehensive search for parameters that correlate with force produced, it may be possible to determine one parameter that is valid for any fin.

VI. Cited Material

[1] C. E. Heine, "Mechanics of flapping fin locomotion in the cownose ray, *Rhinoptera bonasus* (Elasmobranchii: Myliobatidae)," Doctoral Thesis, Department of Zoology, Duke University, 1992.

[2] L. J. Rosenberger, "Pectoral fin locomotion in batoid fishes: Undulation versus oscillation," *Journal of Experimental Biology,* vol. 204, pp. 379-394, Jan 2001.

[3] B. Ahlborn*, et al.*, "Fish without footprints," *Journal of Theoretical Biology,* vol. 148, pp. 521-533, 1991.

[4] S. Michelin and S. G. Llewellyn Smith, "Resonance and propulsion performance of a heaving flexible wing," *Physics of Fluids,* vol. 21, p. 071902, 2009.

[5] P. R. Riggs, "The Use of Biomimetic Fins in Propulsion," Doctoral Thesis, Department of Mechanical Engineering, University of Bath, Bath, 2010.

[6] P. R. Riggs*, et al.*, "Advantages of a Biomimetic Stiffness Profile in Pitching Flexible Fin Propulsion," *Journal of Bionic Engineering,* vol. 7, pp. 113-119, 2010.

[7] M. McHenry*, et al.*, "Mechanical control of swimming speed: stiffness and axial wave form in undulating fish models," *J Exp Biol,* vol. 198, pp. 2293-2305, 1995.

[8] K. M. Collins*, et al.* , "Kinematics of fins with different stiffness profiles", In preparation.

[9] E. J, Anderson, *et al.*. "The Boundary Layer of swimming fish.**"** *The Journal of Experimental Biology* 204, 81–102, 2001.
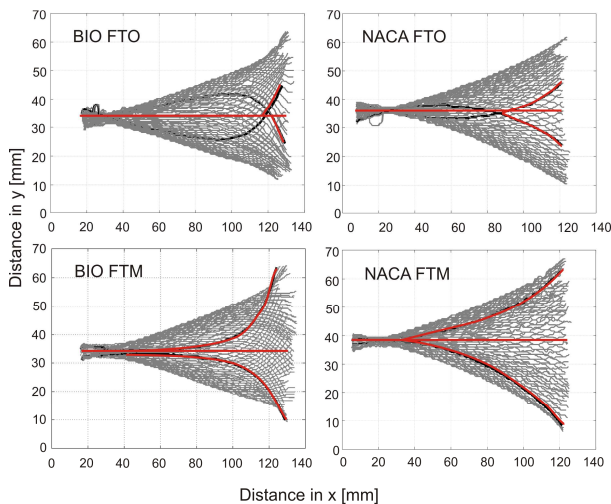
Fig. 7 Calculated midlines of the fins in the FTO (top) and the FTM kinematics (bottom) over one cycle. Midlines are 0.01 s apart. Centreline of a stationary fin shown in red along with the portion of the midline at which the trailing edge angle is at a maximum.